

PACS numbers: 61.05.cp, 68.37.Hk, 73.40.Lg, 73.61.Ga

ELECTROPHYSICAL AND STRUCTURAL PROPERTIES OF *n*-ZnS/*p*-CdTe HETEROJUNCTIONS

D.I. Kurbatov, N.M. Opanasyuk, A.S. Opanasyuk, V.V. Kosyak

Sumy State University,
2, Rimsky-Korsakov Str., 40007, Sumy, Ukraine
E-mail: kurd@ukr.net

Electrophysical and structural properties of ZnS/CdTe film heterojunctions obtained by the sublimation method in quasi-closed volume at different growth conditions have been studied in this work. As a result, the ideality factors, saturation currents, potential barriers and the charge-transport mechanisms of these heterostructures are found. Structural investigations allowed to determine the texture type of the films, their phase composition, the lattice parameters, and the dependence of these parameters on the growth conditions as well. Shown, that on the interface of heterosystems obtained at the substrate temperatures $T_s > 773$ K the solid solutions with certain chemical composition are formed.

Keywords: II-VI FILMS, HETEROJUNCTION, SOLID SOLUTIONS, CRYSTAL STRUCTURE, SCANNING ELECTRON MICROSCOPY, IDEALITY FACTOR, POTENTIAL BARRIER, CHARGE-TRANSPORT MECHANISM.

(Received 18 November 2009, in final form 11 December 2009)

1. INTRODUCTION

n-type cadmium sulfide ($E_g = 2,42$ eV) is a traditional material of the film solar cell (SC) windows based on CIS (CuInSe₂), CIGS (CuIn_{1-x}Ga_xSe₂) and CdTe absorbing layers [1-3]. Presently the maximum conversion efficiency (CE) of the best film SC based on *n*-CdS/*p*-CdTe heterojunctions (HJ) is 16,5% [4-5], but its growth rate slows down. Considered, that increase in SC CE with CdTe absorbing layer can be achieved by the replacement of the optical window material that has stimulated the search of the corresponding wide band gap semiconductors [2, 6, 7]. ZnS is one of such promising materials. Zinc sulfide ($E_g = 3,68$ eV) has substantially larger band gap width in comparison with CdS, and this allows to expand the photosensitivity range of converters and increase their short-circuit currents. In addition, due to the low refraction coefficient ZnS layer can be an anti-reflective coating of SC that increases the number of absorbed photons and, correspondingly, the converter CE. ZnS is a non-toxic ("Cd-free") material because of the absence of heavy metals in its composition, and this is important from the environmental point of view. Properties described above make ZnS films an alternative to CdS layers in modern SC.

The main deficiency of *n*-ZnS/*p*-CdTe HJ is a large mismatch of the lattice parameters of contacting materials (~ 18%) that essentially decreases SC CE. As a rule, efficiency of existing SC does not exceed ~ 4% [2]. But due to the fact that zinc sulfide has the same type of lattice as CdTe and the lattice

forms a number of solid solutions with CdTe, the compensation of difference of the lattice parameters of these materials is possible by the intermediate layer formation on the semiconductor interface. These solid solutions can appear naturally in the diffusion process of the compound components during the time of heterosystem formation or can be artificially created [2].

Electrophysical properties of the multilayer structures play an important role in steady operation and efficiency of solar radiation converters. This paper is devoted to the study of the charge-transport mechanisms through n -ZnS/ p -CdTe HJ and the main parameters they are characterized by. Moreover, we have tried to find the formation conditions of solid solutions described above and additional phases on the interface of contacting materials subject to the modification of the physical and technological conditions of heterosystem production.

2. EXPERIMENTAL TECHNIQUE

To create HJ the chalcogenide films (ZnS and CdTe) were obtained by the sublimation technique in quasi-closed volume [8]. The clean glass plates both with electroconductive transparent ITO layer ($\text{SnO}_2 + \text{In}_2\text{O}_3$) (Fig. 1a) and without it were used as the substrates. Two sets of samples were produced. In the first set CdTe films were deposited on the zinc sulfide layers, and in the second one, contrariwise, the cadmium telluride was used as the bottom layer. Condensation temperature of the optical window material (ZnS) for the samples of the first set varied in the range $T_s = 483$ -785 K, $T_e = 1173$ K. CdTe layers were deposited in the conditions close to the thermodynamically equilibrium ones ($T_s = 823$ K, $T_e = 893$ K) [9].

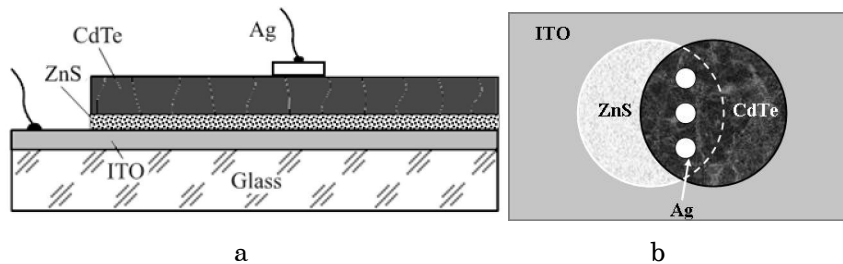


Fig. 1 – Cross-section (a) and the planar geometry (b) of the investigated samples of the first set

CdTe film deposition was simultaneously performed both on the glass substrate and ZnS sublayer (Fig. 1b). This gave a possibility to carry out the comparative analysis of the structural characteristics of CdTe condensates obtained directly on the glass and ZnS sublayer. Upper collector contacts to the multilayer structure were made of silver by the thermal deposition in vacuum.

For diffractometer investigations in order to eliminate lines from the ITO sublayer the reciprocal structures glass/CdTe/ZnS were used, where CdTe layers were deposited in the conditions indicated above and ZnS films at the temperatures $T_s = 523$ -823 K (the second set).

Surface morphology of chalcogenide films was studied by the scanning electron microscopy. Thin silver film was deposited on ZnS layer to provide

the charge drain from the surface. The average grain size (d) in condensates was found by the Jeffries method. The film thickness was measured fractographically. Structural investigations of condensates were done with the X-ray diffractometer DRON 4-07 in Ni-filtered K_{α} -radiation of copper anode. Phase composition, lattice parameter, texture in ZnS and CdTe condensates were found using the technique described in [9, 10].

Investigations of the dark current-voltage characteristics (CVC) of HJ were performed using the high-stable power source AIP B5 120/0,75 at different measurement temperatures ($T = 293\text{-}333\text{ K}$) in vacuum. Temperature control was realized with the automated PID controller OVEN-10M. Then using the standard technique [11] for the CVC analysis the charge-transport features were determined and the main electrophysical parameters of ZnS/CdTe HJ were found.

3. RESULTS DISCUSSION

3.1 Structural investigations

In previous publications [9, 12] we have investigated the influence of the physical and technological condensation conditions in quasi-closed volume on the structural and substructural characteristics of CdTe thin films, and defined the optimal conditions for obtaining layers with the best (from the viewpoint of using in SC) properties (one-phase state, high texturing, large sizes of columnar crystallites and coherent-scattering domains, small micro-deformation level, low concentration of dislocations, etc.): $T_s = 823\text{ K}$ and $T_e = 893\text{ K}$. These regimes were used during CdTe film deposition.

ZnS layers were condensed both at low substrate temperatures ($T_s = 523\text{ K}$) when diffusion can be neglected under deposition on CdTe layer, and at high temperatures ($T_s = 773\text{-}823\text{ K}$) when these processes should be more intensive.

In Fig. 2 we present the typical electron micrographs of CdTe and ZnS film surfaces, which form HJ, and the transition region between them. Samples of the first set were used for the investigation of the condensate morphology.

Microstructure analysis showed that CdTe films on ZnS sublayer consist of the grains of different fractions, both fine (2-3 μm) and coarse (up to 20 μm). The growth steps (see Fig. 2c) are well discerned on the surface of large crystallites. The average grain size of CdTe films is $\sim 7\text{ }\mu\text{m}$. Last values are substantially greater than the grain size in CdTe/glass structures obtained at the same growth conditions [10, 12]. This implies about the certain orienting role of ZnS films. These films have more homogeneous crystal structure (Fig. 2a), the average grain size of which is substantially smaller than in CdTe films and is equal to $\sim 1\text{ }\mu\text{m}$ [13].

Thickness of the obtained CdTe films was $l \sim 10\text{ }\mu\text{m}$, ZnS condensates had smaller thickness $l = (2\text{-}3)\text{ }\mu\text{m}$ since they should be transparent for solar radiation to the CdTe absorbing layer. We have to note a rather good adhesion between the films, which form HJ, in spite of some difference between the linear expansion coefficients of the materials ($6,14 \cdot 10^{-6}\text{ K}^{-1}$ for ZnS and $4,9 \cdot 10^{-6}\text{ K}^{-1}$ for CdTe) [14].

The transition region between ZnS film and CdTe is shown in Fig. 2b. As seen from this figure the certain increase in CdTe grain size in ZnS \rightarrow CdTe

direction is observed. This can be explained by the growth of the chalcogenide thickness. As seen from the HJ cross-section (Fig. 2d) CdTe films have the pronounced columnar growth structure, while ZnS layers consist of a number of grains placed one above the other. On the material interface some interlayer with the modified structure exists, which, as we suggest, is conditioned by the solid solution formation between chalcogenides.

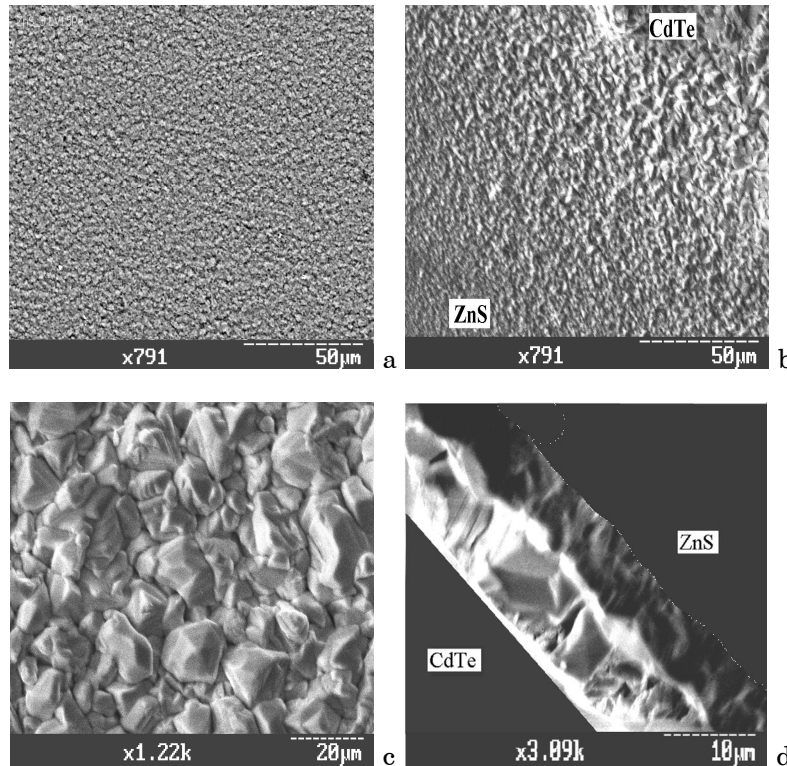


Fig. 2 – Surface microstructure of ZnS films on the glass (a) and of CdTe on ZnS (c); transition region between ZnS film and CdTe (b); ZnS/CdTe HJ cross-section (d). Regimes of ZnS condensation: $T_e = 1173$ K, $T_s = 785$ K; of CdTe: $T_e = 893$ K, $T_s = 823$ K

Typical diffraction patterns obtained from ZnS films on the glass and ZnS/CdTe heterostructures are presented in Fig. 3. For the X-ray investigations the samples of the second set were used. Analysis of the X-ray patterns showed that ZnS films obtained in the temperature range with $T_s < 573$ K on the glass substrates have the sphalerite cubic structure. Hexagonal phase in such condensates is not discovered by the X-ray investigations [15].

As a rule, reflection from (111), (311), (222), (331) planes of the cubic phase is displayed on the diffraction patterns. In most cases (111) peaks are the dominant ones (by intensity) that implies about the pronounced film texture. At $T_s > 573$ K traces of the hexagonal phase (wurtzite) appear in ZnS films, amount of which increases with the condensation temperature growth (Fig. 3a).

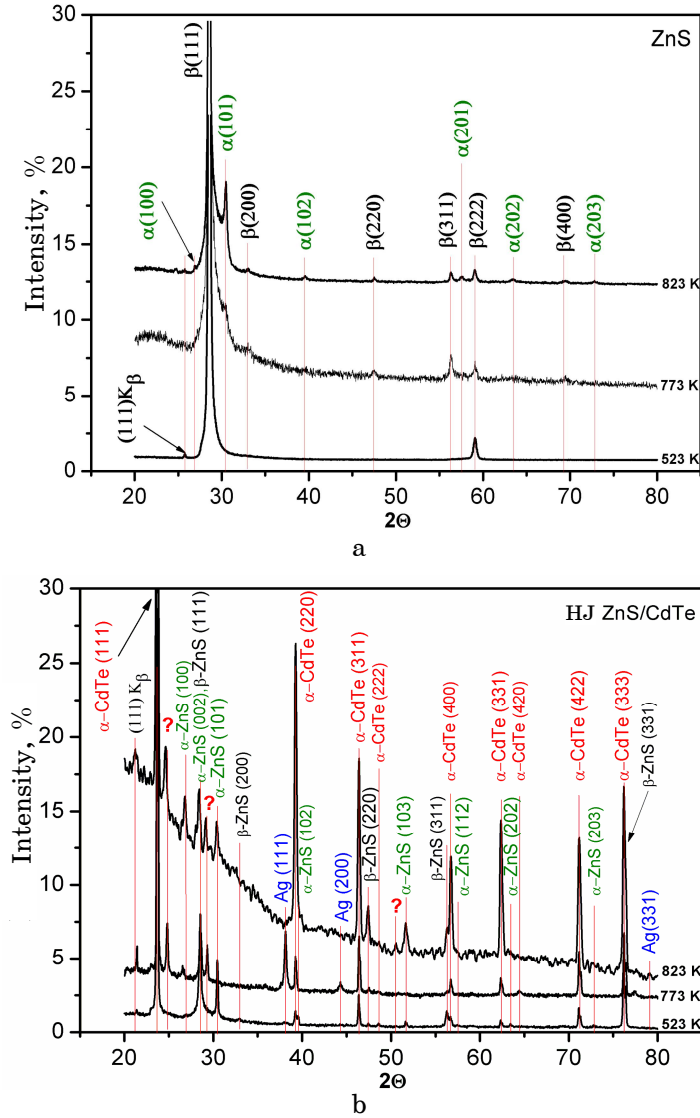


Fig. 3 – Diffraction patterns from ZnS films on the glass (a) and CdTe sublayer (b) obtained at different condensation temperatures

Diffraction patterns from two-layer ZnS/CdTe structures are more complicated than from the single-layer ones, and this makes difficult the phase analysis of the samples. As seen from Fig. 3b, the peaks from crystallographic planes of ZnS and CdTe cubic phases are fixed on these diffraction patterns, and ZnS hexagonal phases are observed there at high condensation temperatures T_s . Detailed interpretation of the X-ray patterns from HJ, where ZnS layer is obtained at $T_s = 823$ K, based on the JCPDS data is presented in Table 1.

Table 1 – Phase analysis of CdTe/ZnS heterosystem (peaks from the possible solid solution (SS) of the compounds are boldfaced)

peak	Investigated sample			JCPDS		α -CdTe	β -ZnS	α -ZnS	SS
	d , nm	2Θ	I	2Θ	I				
1	0,37511	23,70	100	23,76	100	(111)	–	–	–
2	0,36157	24,60	5,16			–	–	–	?
3	0,33261	26,78	4,42	27,08	100	–	–	(100)	–
4	0,31421	28,38	5,62	28,56 (28,69)	100	–	(111)	(002)	–
5	0,30639	29,12	2,85			–	–	–	?
6	0,29397	30,38	3,59	30,70	100	–	–	(101)	–
7	0,22937	39,24	27,35	39,28	60	(220)	–	–	–
8	0,19560	46,38	24,03	46,43	30	(311)	–	–	–
9	0,19171	47,38	4,05	47,51	51	–	(220)	–	–
10	0,18056	50,50	1,57			–	–	–	?
11	0,17698	51,60	3,68	51,90	100	–	–	(103)	–
12	0,16334	56,27	3,59	56,29	30	–	(311)	–	–
13	0,16220	56,70	12,43	56,77	6	(400)	–	–	–
14	0,14876	62,37	22,84	62,40	10	(331)	–	–	–
15	0,13237	71,17	21,45	71,21	10	(422)	–	–	–
16	0,12915	73,22	1,10	73,32	40		–	(203)	–
17	0,12483	76,20	29,93	76,27	4	(333) (511)	–	–	–
18	0,12457	76,42	1,20	76,8	9	–	(331)	–	–

One should pay special attention, that for ZnS at the condensation temperature growth up to $T_s = 773$ K the additional peaks on the angles $2\Theta = 24,60^\circ$ and $29,12^\circ$ appear on the X-ray diffraction patterns. With further increase in the deposition temperature of condensates ($T_s = 823$ K) the intensity of the peaks mentioned above slightly rises, at the same time the appearance of the new peak on the angle $2\Theta = 50,50^\circ$ is fixed.

Diffraction pattern analysis implies that lines on the pointed angles are not connected with reflection from crystallographic planes of chalcogenides ZnS and CdTe and other compounds as well, which could be formed due to the air oxidation of the samples (ZnO, CdO, TeO₂, etc.). In connection with this we can make the assumption about the formation of solid solutions with variable chemical composition on the interface of two chalcogenides, for example, Cd_xZn_{1-x}S, Cd_xZn_{1-x}Te or CdS_xTe_{1-x}, ZnS_xTe_{1-x}. Hence, the fact of the increase in “unknown” peak intensity with the temperature T_s rise becomes clear, since at the condensation of ZnS film on CdTe at high temperatures a more intensive mutual diffusion of semiconductor atoms occurs, and with a large probability this can lead to the appearance of new phases. Taking into account that the diffusion coefficients of metals in II-VI compounds are substantially larger than in chalcogens [17], on the interface first of all one should expect the formation of solid solutions of the type Cd_xZn_{1-x}S or Cd_xZn_{1-x}Te. In the sequel we attempt to determine the approximate composition of these solutions using their lattice parameters and the known data about the dependence of a on x .

We have performed the precise determination of the lattice parameters of ZnS and CdTe layers using the Bradley-Jay and the Nelson-Riley extrapolation methods [18]. Obtained results are presented in Table 2. As seen from this table, the values of a and c found by two different methods correlate well with each other. However, since the values of the lattice parameter obtained by the Nelson-Riley method are more exact, henceforth we will discuss them only.

Table 2 – Precise determination results of the lattice parameters of ZnS and CdTe by the Bradley-Jay and the Nelson-Riley methods

T_s , K	Phase	a , nm	c , nm	a , nm	c , nm	JCPDS
		$a(c) - \cos^2\Theta$		$a(c) - 1/2\cos^2\Theta(1/\sin\Theta + 1/\Theta)$		
523	CdTe	0,64777	–	0,64843	–	$a = 0,64820$
	β -ZnS	0,54083	–	0,54173	–	$a = 0,54060$
	α -ZnS	0,3825	0,6258	0,3830	0,6266	$a = 0,3811$ $c = 0,6234$
773	CdTe	0,64750	–	0,64836	–	$a = 0,64820$
	β -ZnS	0,53866	–	0,54091	–	$a = 0,54060$
823	CdTe	0,64700	–	0,64804	–	$a = 0,64820$
	β -ZnS	0,53859	–	0,54085	–	$a = 0,54060$
	α -ZnS	0,3754	0,6141	0,3806	0,6227	$a = 0,3811$ $c = 0,6234$

Experimental values of the sphalerite lattice parameter in ZnS ($a = 0,54085$ - $0,54173$ nm) and CdTe ($a = 0,64804$ - $0,64843$ nm) films coincide well with the JCPDS data ($a = 0,54060$ nm for ZnS and $a = 0,64820$ nm for CdTe). In this case there is the downward trend in the lattice parameters (for both materials) while the ZnS deposition temperature increases.

For the hexagonal phase of ZnS films the following values of the lattice parameters are obtained: $a = 0,3806$ - $0,3830$ nm and $c = 0,6227$ - $0,6266$ nm ($c/a = 1,64$). These values also correlate well with the JCPDS data: $a = 0,3811$ nm and $c = 0,6234$ nm ($c/a = 1,64$).

Moreover, we have made an attempt to determine the lattice parameter of the solid solution, which, in accordance with the assumption, appears on the interface of chalcogenides. Here considered, that the peak on the angles of $2\Theta = 24,60$ - $24,70^\circ$ belongs to these solutions and is the most intensive one. It is known, that the three-component compound $Cd_xZn_{1-x}Te$ exists in the sphalerite form basically, while compound $Cd_xZn_{1-x}S$ in the wurtzite form [14, 19, 20]. Then the peak on the angles of $2\Theta = 24,60$ - $24,70^\circ$ can belong to either cubic $Cd_xZn_{1-x}Te$ phase (it is the reflection from the plane (111)) or hexagonal $Cd_xZn_{1-x}S$ phase (it is the reflection from the plane (110)). In the first case the lattice parameter in different samples is $a = 0,62215$ - $0,62625$ nm, in the second case it is equal to $a = 0,4175$ - $0,41477$ nm, $c = 0,6786$ - $0,6830$ nm. Assuming that the dependence of the lattice parameters of the solid solutions versus their composition is described by the Vegard's law, it is possible to calculate the approximate value of x [19, 20]. As a result established that reflection on the angles mentioned above can yield solutions of $Cd_xZn_{1-x}Te$

type with $x = 0,76-0,80$ and the sphalerite structure. Solid solutions of $\text{Cd}_x\text{Zn}_{1-x}\text{S}$ type with the wurtzite structure and the derived lattice parameter do not actually exist.

3.2 Electrophysical investigations

Direct branches of the dark CVC of $\text{Ag}/p\text{-CdTe}/n\text{-ZnS}/\text{ITO}$ heterostructures (the first set) plotted in the semi-logarithmic scale are represented in Fig. 4. Dots denote the experimental data, straight lines are produced by the least-squares method using the software package Origin Pro for the numerical analysis. Conductivity type of the condensates obtained in the same growth conditions was defined in our earlier investigations [12, 21]. It was established that ZnS films have the electron conduction, and CdTe films have the hole one.

As investigations showed, the direct branches of CVC at low bias voltages ($U < 1,5$ V) are described by the exponential dependence, while at high external voltages ($U > 20$ V) they are the superlinear ones in the log-log coordinates that is usual for the injection currents. Such features of the current-voltage dependences are typical for HJ with high series resistance, when the contact charge-transport mechanisms are replaced by the volume ones [22-23] with the increase in the bias voltage.

Two sections with different inclination angles to the voltage axis are observed on the HJ CVC presented in the semi-logarithmic scale. In the case of low bias voltages ($U < 0,5$ V) the inclination angle of I - V -dependences decreases with the measurement temperature growth for all investigated samples. This feature is the typical for the thermal activation charge-transport mechanisms through HJ. And contrariwise, independence of the CVC inclination angle to the voltage axis versus the measurement temperature, which is observed at $U > 0,5$ V, is the characteristic of the non-thermal charge-transport mechanisms through heterostructures [11, 22-23]. Known [11], that in the case of the thermal activation charge-transport mechanisms the CVC is described by the following relation:

$$I = I_s \exp(qU/nkT), \quad (1)$$

where I is the current through HJ; I_s is the saturation current; q is the electron charge; U is the bias voltage applied to the structure; n is the HJ ideality factor; k is the Boltzmann constant; T is the measurement temperature.

In turn, the saturation current can be found as

$$I_s = I_{0s} \exp(qU_{k0}/nkT), \quad (2)$$

where U_{k0} is the potential barrier height of the junction in the absence of the bias voltage.

In the case of the non-thermal charge-transport mechanisms through HJ the direct branch of the CVC is described by expression [11]

$$I = I_s \exp(\alpha U), \quad (3)$$

where

$$I_s = I_{0s} \exp(\beta T). \quad (4)$$

Here I_{0s} , α , β are the constants, which do not depend on U and T .

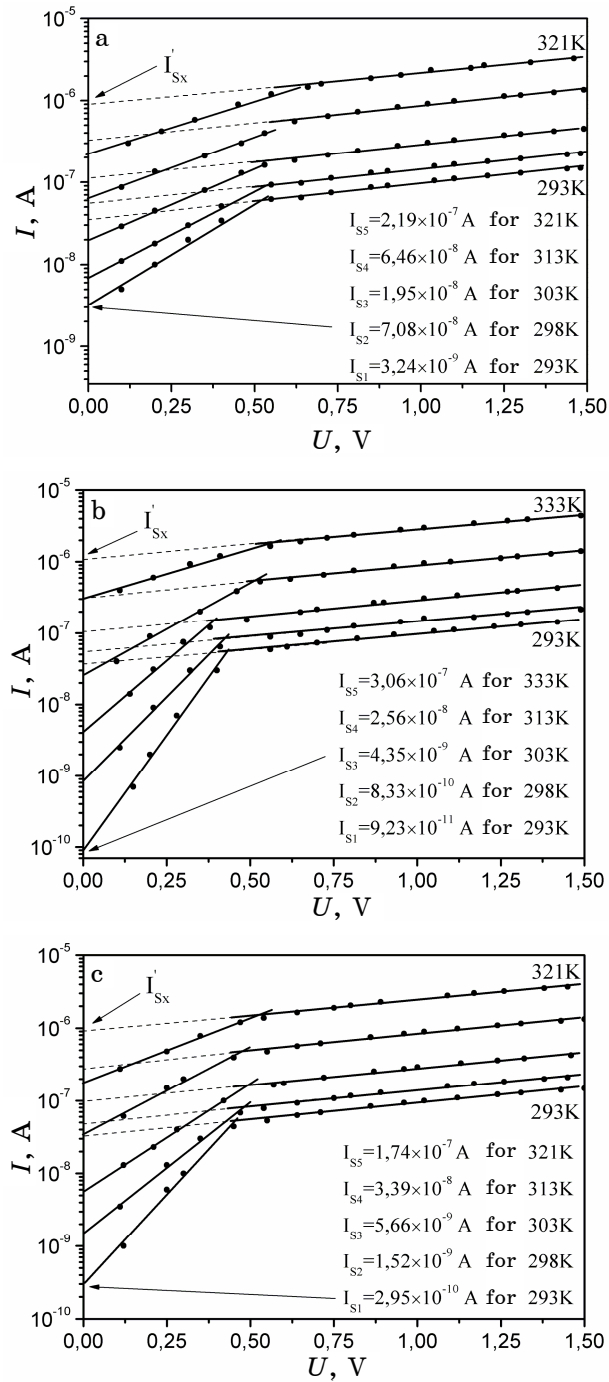


Fig. 4 – Direct branches of the *n*-ZnS/*p*-CdTe HJ CVC obtained at different measurement temperatures. Regimes of ZnS film condensation: $T_s = 483 K$ (a), $T_s = 623 K$ (b) and $T_s = 785 K$ (c)

We have to note, that the charge-transport mechanism through HJ is substantially defined by the state of semiconductor interface. Known [11, 17, 22-23], that in the case of the lattice parameter mismatch for the materials forming the heterosystem, which exceeds 4%, the electrical properties of HJ are completely defined by the surface states.

To determine the main electrophysical parameters of heterosystems the temperature-dependent sections of the CVC were linearized in the $\text{Lg}I_s-1/T$ coordinates, while the temperature-non-dependent sections in the $\text{Lg}I_s-T$ ones (Fig. 5). Then using relations (2) and (4) from the obtained lines by their inclination angles and values, which were intercepted on the current axis, the specified values of the constants n , U_{k0} , α and β were found.

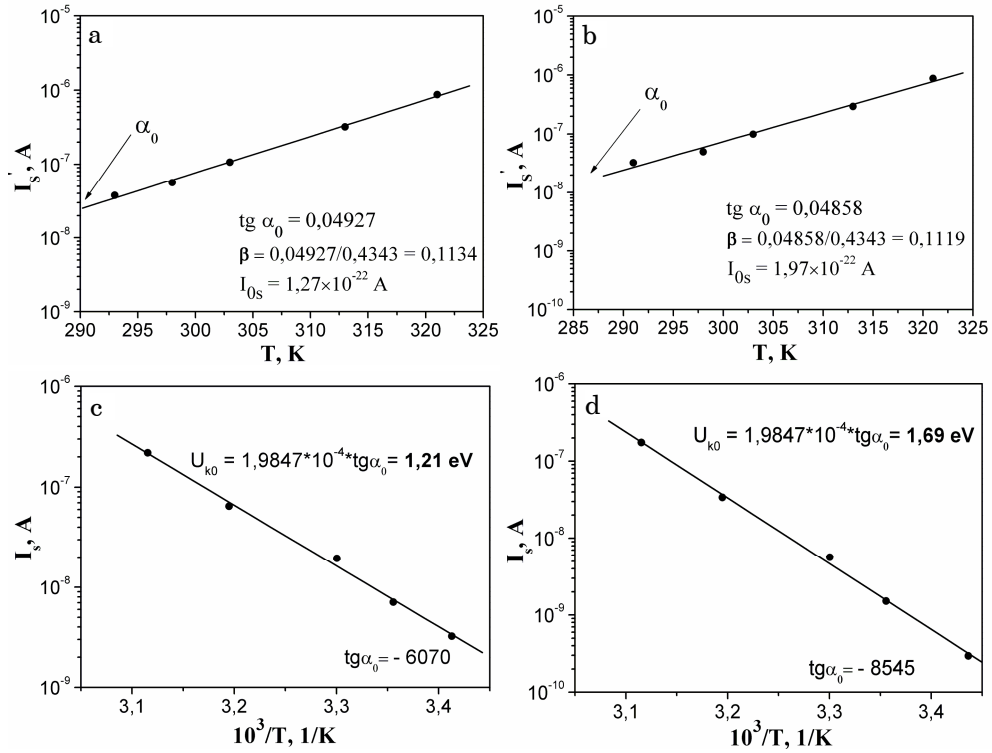


Fig. 5 – Typical temperature dependences of the saturation current I_s for $U > 0,5$ V (a, b) and $U < 0,5$ V (c, d). Regimes of ZnS film condensation: $T_s = 483$ K (a, c), $T_s = 785$ K (b, d)

Calculation results are integrated in Table 3. As seen from this table, the ideality factor of investigated HJ varies in the range $n = 2,70-7,04$. It has the lowest value $n = 2,70$ in systems at $T_s = 623$ K. These results coincide with those obtained by the authors of [24].

Values of the potential barrier height on HJ $U_{k0} = (1,21-1,69)$ eV (found from the CVC) correlate well with the values calculated theoretically: $U_{k0}(\text{th.}) = \Phi_{\text{ZnS}} - \Phi_{\text{CdTe}} = 7,0-5,7 = 1,30$ eV (Φ is the electron work function) [25, 26]. In this case increase in U_{k0} is observed with the growth of ZnS film

deposition temperature. This can be conditioned by the change in the phase composition of ZnS layer and the state of semiconductor interface.

Parameters α and β depend weakly on the physical and technological conditions of the HJ production and vary in the range $\alpha = 0,951-1,032$ and $\beta = 0,084-1,134$. Joint analysis of the CVC, the temperature dependence of the saturation current I_s and the constants, which characterize the charge-transport in the structure, implies that in n -ZnS/ p -CdTe HJ for the bias voltages $U < 0,5$ V the emission-recombination charge-transport mechanism is realized, and for $U > 0,5$ V it is replaced by the tunnel-recombination one.

Table 3 – Main electrophysical parameters of n -ZnS/ p -CdTe HJ

ZnS condensation temperature T_s , K	Ideality factor n	Potential barrier height U_{k0} , eV	Parameter α	Parameter β
483	7,04	1,21	0,954	0,1134
623	2,70	1,57	0,951	0,0840
785	3,50	1,69	1,032	0,1119

4. CONCLUSIONS

In the wide range of the physical and technological condensation conditions n -ZnS/ p -CdTe HJ are obtained by the sublimation method in quasi-closed volume. The element composition of heterostructures is studied, the type of their texture and the lattice parameters of the materials are determined. Showed, that the presence of ZnS sublayer leads to the increase in the grain size of CdTe condensates deposited in the quasi-equilibrium conditions. This implies about the partial heteroepitaxial growing of CdTe layer on ZnS sublayer. Possibility of the solid solution formation on the material interface at high temperatures of the film condensation is confirmed. As a result of the calculations it is established that in ZnS/CdTe system the solid solutions of $Cd_xZn_{1-x}Te$ type, where $x = 0,76-0,80$, with the sphalerite structure are formed.

Investigations of the dark CVC of heterosystems at different measurement temperatures allowed to determine the ideality factors of HJ, their saturation currents, the potential barrier height and the charge-transport mechanisms. Established, that for the bias voltages $U < 0,5$ V the emission-recombination charge-transport mechanism is realized, which for $U > 0,5$ V is replaced by the tunnel-recombination one.

REFERENCES

1. D. Hariskos, S. Spiering, M. Powalla, *Thin Solid Films* **480-481**, 99 (2005).
2. I.O. Olageji, L. Chow, C.S. Ferekides, V. Viswanathan, Z. Zhao, *Sol. Energ. Mat. Sol. Cel.* **61**, 203 (2000).
3. W.K. Metzger, I.L. Repins, M.A. Contreras, *Appl. Phys. Lett.* **93**, 022110 (2008).
4. A. Bosio, N. Romeo, S. Mazzamuto, V. Canevari, *Prog. Cryst. Growth. Ch.* **52**, 247 (2006).
5. X. Wu, *Sol. Energy* **6**, 803 (2004).
6. G. Contreras-Puente, O. Vigil, M. Ortega-Lypez, *Thin Solid Films* **361-362**, 378 (2000).
7. R. Venugopal, B.K. Reddy, D.R. Reddy, *Mat. Chem. Phys.* **55**, 36 (1998).
8. Y.P. Venkata Subbaiah, P. Prathap, M. Devika, *Physica B* **365**, 240 (2005).

9. D. Kurbatov, V. Kosyak, A. Opanasyuk, *Integr. Ferroelectr.* **103**, 32 (2008).
10. D. Kurbatov, A. Opanasyuk, H. Khlyap, *phys. status solidi (a)* **206**, 1549 (2009).
11. B.L. Sharma, R.K. Purohit, *Poluprovodnikovye geteroperehody* (M.: Sov. radio: 1979).
12. V.V. Kosyak, M.M. Kolesnik, A.S. Opanasyuk, *J. Mater. Sci.-Mater. El.* **19**, S375 (2008).
13. D. Kurbatov, A. Opanasyuk, A. Kramchenkov, *Semiconductor Phys. Quantum Electron. Optoelectron.* **11**, 252 (2008).
14. N.N. Berhenko, V.E. Krevs, V.G. Sredin, *Poluprovodnikovye tverdye rastvory i ih primenenie: Spravochnye tablitsy* (M.: Voenizdat: 1982).
15. A.G. Balogh, S.M. Duvanov, D.I. Kurbatov, *Photoelectronics* **17**, 134 (2008).
16. *Selected powder diffraction data for education straining (Search manual and data cards)* (Published by the International Centre for diffraction data, USA: 1988).
17. I.P. Kalinkin, V.B. Aleskovskiy, *Epitaksial'nye plinki soedineniy A_2B_6* (Leningrad: Izd-vo LGU: 1978).
18. B.E. Warren, *X-ray Diffraction* (New York: Dover: 1990).
19. F.E.H. Hassan, B. Amrani, F. Bahsoun, *Physica B* **391**, 363 (2007).
20. J.H. Lee, W.C. Song, J.S. Yi, K.J. Yang, W.D. Han, J. Hwang, *Thin Solid Films* **431-432**, 349 (2003).
21. D. Kurbatov, V. Kosyak, A. Opanasyuk, V. Melnik, *Physica B* **404**, 5002 (2009).
22. A.V. Simashkevich, *Geteroperehody na osnove poluprovodnikovyyh soedineniy A_2B_6* (Kishinev: Shtiintsa: 1980).
23. A. Farenbruk, R. Bjub, *Solnechnye elementy. Teoriya i eksperiment* (M.: Energoatomizdat: 1987).
24. S.K.J. Al-Ani, A.Kh. Ba-Yashoot, M.N. Makadsi, *Turk. J. Phys.* **31**, 259 (2007).
25. X.S. Fang, Y. Bando, G.Z. Shen, C.H. Ye, U.K. Gautam, P.M.F.J. Costa, C.Y. Zhi, C.C. Tang, D. Golberg, *Adv. Mater.* **19**, 2593 (2007).
26. A. Alnajjar, S. Abdul Jawad, N. Yusuf, *Renew. Energ.* **27** No3, 417 (2002).